

Chemical shift and zone-folding effects on the energy gaps of GaAs-AlAs (001) superlattices

S. B. Zhang

*Department of Physics, University of California, and Materials Sciences Division,
Lawrence Berkeley Laboratory, Berkeley, California 94720
and Xerox Palo Alto Research Center, 3333 Coyote Hill Road, Palo Alto, California 94304*

Marvin L. Cohen and Steven G. Louie

*Department of Physics, University of California, and Materials Sciences Division,
Lawrence Berkeley Laboratory, Berkeley, California 94720*

(Received 1 November 1990)

The chemical shift and zone-folding effects obtained from quasiparticle calculations for ultrathin GaAs-AlAs superlattices are incorporated within a Kronig-Penny model for superlattices of the arbitrary lattice period. We determine that superlattices with lattice periods in the range of 3×3 to 9×9 have an X -derived pseudodirect gap. This result explains both the results from first-principles calculations for ultrathin superlattices and those from experiments for a broader lattice period.

There has been a great deal of interest in short-period superlattices because these superlattices often possess tunable electronic properties and hence have potential applications. GaAs-AlAs is a good example¹⁻¹³ and it serves as a prototype for investigation. GaAs has a direct gap at Γ , whereas AlAs has an indirect gap at X , which is 0.7 eV larger. Because of the ~ 0.5 -eV valence-band offset¹⁴ and because the confinement potential for the GaAs Γ state in a GaAs-AlAs superlattice (~ 1 eV) is much larger than the confinement potential for the AlAs X state (~ 0.3 eV), direct to indirect (or pseudodirect) transitions are expected to occur for certain lattice periods. This view is supported by previous effective-mass (EM) model calculations designed to study confinement effects.^{13,15,16} Experiments for short-period superlattices^{9,10,17} also show some evidence for direct to indirect transition. Recently, a first-principles quasiparticle calculation for ultrathin superlattices¹⁸ has been done. The results disagree with the EM models and show that the extremely thin 1×1 and 2×2 superlattices are direct rather than indirect. In this paper, the differences between the two calculations are examined. We find that they are caused by short-range chemical effects and other interface-related effects which are ignored in the EM models.

Our model makes use of results from first-principles quasiparticle calculations for ultrathin superlattices of GaAs-AlAs which were designed to examine microscopic features of the interface (Ref. 18) and results from the Kronig-Penny model for confinement effects for arbitrary lattice period for k points near the Brillouin-zone center.

Within the Kronig-Penny model, the Hamiltonian \hat{H} contains the kinetic energy and a periodic step potential with infinitely sharp boundaries at the interfaces. The confinement energy ϵ and the wave function ψ are given by solving the Schrödinger equation,

$$\hat{H}\psi = \epsilon\psi. \quad (1)$$

Equation (1), together with the boundary conditions pro-

posed by Bastard,¹⁵ yields an equation for the lowest confinement energy,¹⁶

$$\tan \left[\frac{l_a}{2} (m_a \epsilon)^{1/2} \right] - \left[\frac{m_a}{m_b} \left[\frac{V}{\epsilon} - 1 \right] \right]^{1/2} \times \tanh \left[\frac{l_b}{2} [m_b (V - \epsilon)]^{1/2} \right] = 0, \quad (2)$$

where l_a and l_b are the lattice thicknesses of the potential well and barrier, respectively, m_a and m_b are the effective masses, and V is the corresponding barrier height in Rydberg atomic units. The optical energy gaps for the superlattices are the sum of the confinement energies of both conduction- and valence-band states given by Eq. (2) and the corresponding bulk energy gaps. The effective masses used here are from Ref. 13 and the zero-temperature lattice constant of GaAs is assumed.¹⁹

As discussed in Ref. 18, the interfacial bonding effect (or chemical shifts) of the Γ_{1c} state is the major cause for the direct gap change from the EM result for at least the 1×1 and 2×2 lattices. It arises from the difference between the Ga and Al ionic potentials. Since the Γ_{1c} state is an on-site antibonding state, electrons in this state experience stronger repulsive Al potentials and hence are pushed away from AlAs. In Fig. 1 the average charge along the lattice axis for the Γ_{1c} state for a 3×3 lattice calculated using the local-density approximation (LDA) is shown. Figure 1 also displays the charge calculated from an envelope-function approach. In the latter, wave functions are constructed from corresponding bulk states modulated by the envelope functions from the Kronig-Penny model.²⁰ Mixing between the Γ_{1c} state and the folded X_{1c} state is ignored here because the overlap is small (e.g., less than 1% for a 3×3 lattice). For comparison, the result for the X_{1c} state is also shown. From Fig. 1, the envelope-function approximation works reasonably well for charge distributions a few atomic layers away from the interface. Hence, the change in the interfacial

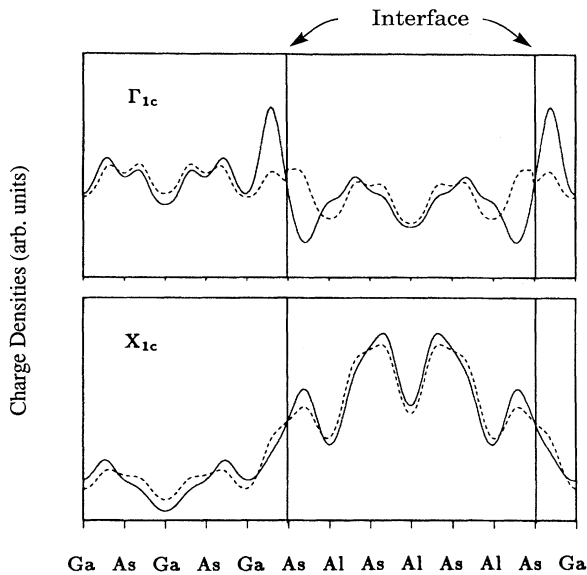


FIG. 1. The average charge densities along the z direction for the Γ_{1c} -derived state and for the X_{1c} -derived state for a 3×3 lattice. The solid lines are the LDA results and the dashed lines are the results from the envelope-function approach.

bonding when going beyond EM theory for the Γ_{1c} state arises, to a large extent, from charge-density changes on an atomic scale.

In order to include in a simple fashion the chemical shift for the Γ_{1c} state in the Kronig-Penny model, we propose that the net transfer of charge to the GaAs interfacial monolayer may be thought of as arising from an extra effective (attractive) potential of the form

$$V_{\text{eff}} = -AV_0P_I, \quad (3)$$

where P_I is a projection operator for the GaAs interfacial monolayer and A is a constant to be determined from our 1×1 and 2×2 quasiparticle calculations. The change in the confinement energy for arbitrary period is then

$$\delta E = \langle \psi | V_{\text{eff}} | \psi \rangle = -AV_0 \langle \rho_{\text{GaAs}} \rangle_{\text{ML}}, \quad (4)$$

where $\langle \rho_{\text{GaAs}} \rangle_{\text{ML}}$ is the charge per monolayer within the effective-mass Kronig-Penny model.

Our results for the direct energy gaps together with the data from the photoluminescence excitation and resonant Raman scattering measurements near zero temperature are shown in Fig. 2. The agreement between theory and experiment is good. In most cases, the deviation is only a few hundredths of an eV and is within the experimental uncertainties. It appears, however, that the results of Jiang and co-workers⁴ exhibit an extra gap minimum near 3×3 . This could be caused by imperfect growth of samples. For example, our calculation gives an energy gap of 2.16 eV when a 3×3 lattice is assumed and 2.07 eV when a $10\text{-}\text{\AA}$ – $8\text{-}\text{\AA}$ superlattice dimension is used. The latter case is also classified in experiment as a 3×3 lattice. The result of Jiang and co-workers of 2.11 eV falls between the calculated values for the above two geometries. For comparison, energy gaps from the

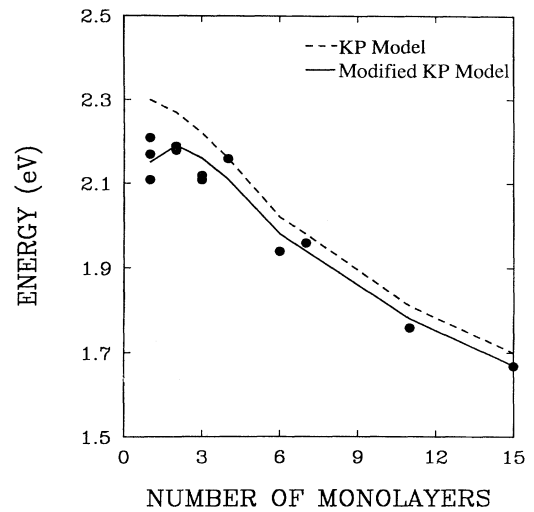


FIG. 2. Calculated direct gaps as a function of lattice periods. The solid circles are the photoluminescence excitation data (Refs. 4–7, 10, and 11).

Kronig-Penny model are also shown in Fig. 2, which are consistently larger than the experimental results and the results from our model. The difference increases as the layer thickness decreases.

A notable feature of the present model is that the direct gap reaches its maximum value near the 2×2 lattice instead of having a monotonic decrease as the layer thickness increases as predicted by the Kronig-Penny model. This trend agrees with the recent first-principles quasiparticle calculations.¹⁸ The maximum position which occurs near the 2×2 lattice is consistent with the fact that the interfacial bonding is short ranged.

In Fig. 3 the calculated direct and pseudodirect gaps

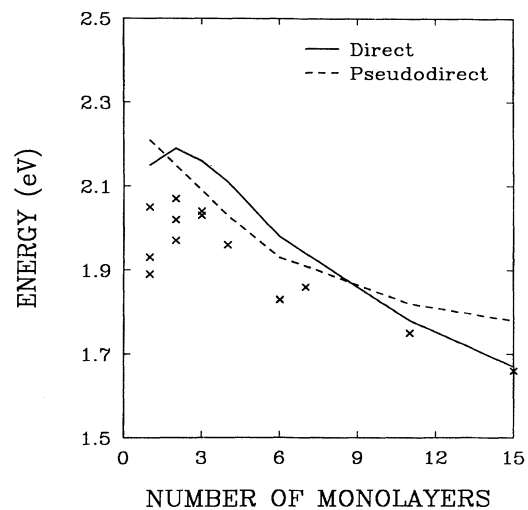


FIG. 3. Calculated direct and pseudodirect gaps as a function of lattice periods. The crosses are the minimum gaps measured by photoluminescence experiment (Refs. 2–5, 8–10, and 17).

and the photoluminescence data are shown to display the present experimental situation. We note that the results of the photoluminescence experiment, in which the minimum gap is measured, are different from the photoluminescence excitation experiment for direct gaps (Fig. 2). To obtain a reasonable estimate for the pseudodirect gap, we have proceeded in the following way. We first calculated the gap for the folded X_{1c} state from the Kronig-Penny model and then included a correction term which is based on the quasiparticle calculation for ultrathin superlattices. The correction term takes care of the many-body effects related to the Brillouin-zone folding. It oscillates somewhat between even and odd lattices. From Ref. 18, this term is 0.1 eV for a 1×1 lattice. It gets smaller for larger lattice periods and eventually becomes negligible when the interfacial region is only a small portion of the superlattice. Hence, we approximate the correction by

$$\delta\varepsilon = 0.1\rho_{\text{int}} \text{ (eV)}, \quad (5)$$

where ρ_{int} is the total charge within the interfacial subcell (two monolayers) and ρ is normalized to one electron per supercell.

From Fig. 3 we determine that the pseudodirect gap is below the direct gap in the approximate lattice range from 2×2 to 9×9 . Available experimental data support the overall features of our calculation. The lower-energy peaks in photoluminescence for $n = m \geq 10$ are in good agreement with the calculated direct gaps whereas the data for the superlattices between 3×3 and 7×7 are closer to and track the calculated *pseudodirect* gaps. The fact that these values are consistently smaller than the theory (Fig. 3) suggests that it is not the folded $X_{1c,z}$ pseudodirect state but is the unfolded $X_{1c,xy}$ indirect states being measured in these experiments. The $X_{1c,xy}$ states are a few hundredths of an eV below the $X_{1c,z}$ state in the short lattice range as suggested by the recent quasiparticle calculations¹⁸ and determined by experiments.^{9,10} In any case, the photoluminescence data for the 1×1 and

2×2 lattices do not match the theoretical gaps with the experimental values showing large scattered values (within 0.15 eV). We have proposed alternative assignments for these transitions which are discussed in Ref. 18. Briefly, these transitions are related to the indirect transition to the \bar{R} state for the 1×1 lattice and to the direct transitions within local GaAs-rich structures for the 2×2 lattice. Recently, photoacoustic saturation (PAS) spectroscopy was used to study the band structure of GaAs-AlAs ultrathin superlattices with somewhat less accuracy.¹⁷ While the PAS results agree with the Kronig-Penny model, the agreement with the photoluminescence excitation spectrum for ultrathin superlattices (see Fig. 2) is poor. Discrepancies among different experiments may be caused by cation disorder. To explore such an effect, we have performed a virtual-crystal-type (VCA) calculation for GaAlAs alloys.¹⁸ As expected, the result for alloy ($x = 50\%$) appears very close to that given by the Kronig-Penny model for a 1×1 superlattice.

In conclusion, we have examined the range and magnitude of the deviations from the actual situation for the effective-mass model for GaAs-AlAs superlattices (with the Kronig-Penny model as our example). The deviations are found to arise mainly from an interfacial chemical bonding effect for the Γ_{1c} state and a zone-folding effect for the X_{1c} state. Using this model and our quasiparticle calculations, we predict that the GaAs-AlAs superlattices are pseudodirect (or indirect) in the approximate lattice range from 3×3 to 9×9 .

The work at Berkeley was supported by National Science Foundation Grant No. DMR8818404 and by the Director, Office of Energy Research, Office of Basic Energy Sciences, Materials Sciences Division of the U.S. Department of Energy under Contract No. DE-AC03-76SF00098. S.G.L. acknowledges support from the J. S. Guggenheim Foundation. S.B.Z. at Xerox Palo Alto Research Center was supported by the U.S. Office of Naval Research through Contract No. N00014-82-C-0244.

¹E. Caruthers and P. J. Lin-Chung, Phys. Rev. Lett. **38**, 1543 (1977).

²A. Ishibashi, Y. Mori, M. Itabashi, and M. Watanabe, J. Appl. Phys. **58**, 2691 (1985).

³T. Isu, D. S. Jiang, and K. Ploog, Appl. Phys. A **43**, 75 (1987).

⁴D. S. Jiang, K. Kelting, T. Isu, H. J. Queisser, and K. Ploog, J. Appl. Phys. **63**, 845 (1988).

⁵J. Nagle, M. Garriga, W. Stolz, T. Isu, and K. Ploog, J. Phys. C **5**, 495 (1987).

⁶M. Alouani, S. Gopalan, M. Garriga, and N. E. Christensen, Phys. Rev. Lett. **61**, 1643 (1988).

⁷M. Garriga, M. Cardona, N. E. Christensen, P. Lautenschlager, T. Isu, and K. Ploog, Phys. Rev. B **36**, 3254 (1987).

⁸M. Cardona, T. Suemoto, N. E. Christensen, T. Isu, and K. Ploog, Phys. Rev. B **36**, 5906 (1987).

⁹E. Finkman, M. D. Sturge, and M. C. Tamargo, Appl. Phys. Lett. **49**, 1299 (1986).

¹⁰E. Finkman, M. D. Sturge, M. H. Meynadier, R. E. Nahory, M. C. Tamargo, D. M. Hwang, and C. C. Chang, J. Lumin. **39**, 57 (1987).

¹¹M. H. Meynadier, R. E. Nahory, J. M. Worlock, M. C. Tamargo, J. L. de Miguel, and M. D. Sturge, Phys. Rev. Lett. **60**, 1338 (1988).

¹²N. Kobayashi, T. Toriyama, and Y. Horikoshi, Appl. Phys. Lett. **50**, 1811 (1987).

¹³G. Danan, B. Etienne, F. Mollot, R. Planel, A. M. Jean-Louis, F. Alexandre, B. Jusserand, G. Le Roux, J. Y. Marzin, H. Savary, and B. Sermage, Phys. Rev. B **35**, 6207 (1987).

¹⁴S. B. Zhang, D. Tománek, S. G. Louie, M. L. Cohen, and M. S. Hybertsen, Solid State Commun. **66**, 585 (1988).

¹⁵G. Bastard, Phys. Rev. B **24**, 5693 (1981).

¹⁶H. S. Cho and P. R. Prucnal, Phys. Rev. B **36**, 3237 (1987).

¹⁷R. Cingolani, L. Baldassarre, M. Ferrara, M. Lugará, and K. Ploog, Phys. Rev. B **40**, 6101 (1989).

¹⁸S. B. Zhang, M. S. Hybertsen, S. G. Louie, M. L. Cohen, and D. Tománek, *Phys. Rev. Lett.* **63**, 1495 (1989).

¹⁹*Numerical Data and Functional Relationships in Science and Technology—Crystal and Solid State Physics*, edited by O. Madelung, Landolt-Bornstein, Vol. 17A (Springer, Berlin,

1984).

²⁰The potential barrier is adjusted so that the integrated charge in the bulklike regions, defined as the double monolayers around the centers of each subcell, matches the charge given by a calculation based on the LDA.